JACS
JOURNAL OF THE AMERICAN CHEMICAL SOCIETY
Article
pubs.acs.org/JACS

Efficient Two-Electron Reduction of Dioxygen to Hydrogen Peroxide with One-Electron Reductants with a Small Overpotential Catalyzed by a Cobalt Chlorin Complex

Kentaro Mase,[†] Kei Ohkubo,[†] and Shunichi Fukuzumi*[,†,‡]

[†]Department of Material and Life Science, Graduate School of Engineering, ALCA, Japan Science and Technology Agency (JST), Osaka University, Suita, Osaka 565-0871, Japan

[‡]Department of Bioinspired Science, Ewha Womans University, Seoul 120-750, Korea

Supporting Information

ABSTRACT: A cobalt chlorin complex ($Co^{II}(Ch)$) efficiently and selectively catalyzed two-electron reduction of dioxygen (O_2) by one-electron reductants (ferrocene derivatives) to produce hydrogen peroxide (H_2O_2) in the presence of perchloric acid ($HClO_4$) in benzonitrile (PhCN) at 298 K. The catalytic reactivity of $Co^{II}(Ch)$ was much higher than that of a cobalt porphyrin complex ($Co^{II}(OEP)$, OEP^{2-} = octaethylporphyrin dianion), which is a typical porphyrinoid complex. The two-electron reduction of O_2 by 1,1′-dibromoferrocene (Br_2Fc) was catalyzed by $Co^{II}(Ch)$, whereas virtually no reduction of O_2 occurred with $Co^{II}(OEP)$. In addition, $Co^{II}(Ch)$ is more stable than $Co^{II}(OEP)$, where the catalytic turnover number (TON) of the two-electron reduction of O_2 catalyzed by $Co^{II}(Ch)$ exceeded 30000. The detailed kinetic studies have revealed that the rate-determining step in the catalytic cycle is the proton-coupled electron transfer reduction of O_2 with the protonated $Co^{II}(Ch)$ ($[Co^{II}(ChH)]^+$) that is produced by facile electron-transfer reduction of $[Co^{III}(ChH)]^{2+}$ by ferrocene derivative in the presence of $HClO_4$. The one-electron-reduction potential of $[Co^{III}(Ch)]^+$ was positively shifted from 0.37 V (vs SCE) to 0.48 V by the addition of $HClO_4$ due to the protonation of $[Co^{III}(Ch)]^+$. Such a positive shift of $[Co^{III}(Ch)]^+$ by protonation resulted in enhancement of the catalytic reactivity of $[Co^{III}(ChH)]^{2+}$ for the two-electron reduction of O_2 with a lower overpotential as compared with that of $[Co^{III}(OEP)]^+$.

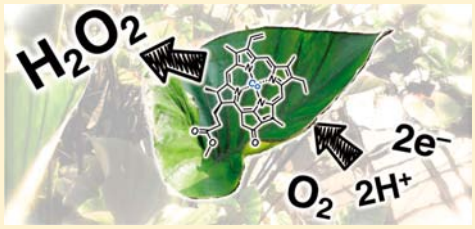

INTRODUCTION

Hydrogen peroxide is one of the most versatile and environmentally benign oxidizing reagents produced in large scale in industry, with various applications including pulp and paper bleaching.[1,2] Hydrogen peroxide is also a promising candidate as a sustainable energy carrier,[3,4] because it has high energy density and emits no CO_2, which is regarded as a greenhouse gas causing serious environmental issues. Hydrogen peroxide fuel cells, which emit only water and oxygen after power generation, have recently been developed, and the cell performance has been improved significantly.[4−9] Currently hydrogen peroxide is manufactured in industry by the autoxidation of a 2-alkylanthrahydroquinone to the corresponding 2-alkylanthraquinone (the so-called anthraquinone process).[10] This process requires hydrogen as a reductant and a noble metal such as palladium to regenerate the anthrahydroquinone. The cost of the anthraquinone process depends heavily on effective recycling of the anthraquinone, extraction solvents, and the noble-metal hydrogenation catalyst, which are all quite expensive.

Alternatively, production of hydrogen peroxide has been extensively studied by the electrocatalytic two-electron reduction of oxygen, which is abundant in air.[4,11−18] Base-metal catalysts such as cobalt,[11,13−32] iron,[33−36] and copper[37−39] complexes have been employed for the two-electron and four-electron reduction of O_2. Monomeric cobalt porphyrins and cobalt phthalocyanines act as efficient catalysts for the selective two-electron reduction of O_2 by ferrocene derivatives in the presence of an acid.[11,19,21] An increase of the one-electron-reduction potential of cobalt(III) complexes is required to reduce the overpotential for the two-electron reduction of O_2. However, when the one-electron reduction potentials of cobalt(III) complexes are too positive, the Co(II) complexes may not be able to reduce O_2. The overpotential of the two-electron reduction of O_2 with cobalt complexes has not been optimized yet. The stability of the catalyst under the acidic conditions should also be improved because demetalation from a macrocyclic ligand results in inactivation of the catalyst.

In general, the stability of a metal complex with a porphyrinoid ligand in the presence of acid depends on two factors.[40−43] One is the core size and rigidity of a macrocyclic ligand, because a low-valent metal ion, which is produced in a catalytic cycle, is difficult to accommodate in a macrocyclic ligand due to its large ionic radius and low electrostatic interaction. The core size of the chlorin ligand is larger than that of porphyrin because the chlorin ligand is more flexible than the porphyrin in accommodating the low-valent metal ion. The other is the nucleophilicity of the core nitrogen atoms, which is responsible for electrophilic attack of an

Received: December 13, 2012
Published: January 23, 2013

   dx.doi.org/10.1021/ja312199h | J. Am. Chem. Soc. 2013, 135, 2800−2808

incoming proton. The nucleophilicity of a macrocyclic ligand diminishes, accompanied by the electron density of the macrocyclic ligand, which is associated with saturation of C−C bonds in the pyrrole rings (porphyrin > chlorin). In this regard, Co^{II}(Ch) possesses advantages for the stability in an acidic solution, leading to efficiency and durability for the catalytic two-electron reduction of O_2.

We report herein that a cobalt(II) chlorin complex (Co^{II}(Ch)) catalyzes efficiently the two-electron reduction of O_2 with a series of ferrocene derivatives as an electron donor in the presence of perchloric acid ($HClO_4$) in PhCN. The electrocatalytic reduction of O_2 with Co^{II}(Ch) occurs with high durability in the acidic solution and a small overpotential in comparison with macrocyclic ligands already reported.[4,13] The catalytic mechanism for the selective two-electron reduction of O_2 by ferrocene derivatives is clarified on the basis of a detailed kinetic study.

EXPERIMENTAL SECTION

General Procedure. Chemicals were purchased from commercial sources and used without further purification, unless otherwise noted. Benzonitrile (PhCN) used for spectroscopic and electrochemical measurements was distilled over phosphorus pentoxide prior to use.[44] Cobalt chlorin (Co^{II}(Ch)) was synthesized by the published method (see the Supporting Information for details).[45,46] Ferrocene (Fc), 1,1′-dimethylferrocene (Me_2Fc), octamethylferrocene (Me_8Fc), bromoferrocene (BrFc), and 1,1′-dibromoferrocene (Br_2Fc) were purchased commercially and purified by sublimation or recrystallization from ethanol. Tetra-*n*-butylammonium hexafluorophosphate ($TBAPF_6$) was twice recrystallized from ethanol and dried in vacuo prior to use. ^1H NMR spectra (300 MHz) were recorded on a JEOL AL-300 spectrometer at room temperature, and chemical shifts (ppm) were determined relative to tetramethylsilane (TMS). MALDI-TOF-MS measurements were performed on a Kratos Compact MALDI I (Shimadzu) using dithranol as a matrix. UV−vis spectroscopy was carried out on a Hewlett-Packard 8453 diode array spectrophotometer at room temperature using 1 cm cells.

Spectroscopic Measurements. The protonation equilibrium constants between Co^{II}(Ch) and $[Co^{II}(ChH)]^+$ and between $[Co^{III}(Ch)]^+$ and $[Co^{III}(ChH)]^{2+}$ were determined by using the Hill equation, which analyzes changes in absorption spectra during the titration as a function of the concentration of an added acid.[47] The amount of hydrogen peroxide (H_2O_2) formed was determined by titration with iodide ion: a dilute CH_3CN solution (2.0 mL) of the product mixture (40 μL) was treated with an excess amount of NaI, and the amount of I_3^- formed was determined by the absorption spectrum (λ_{max} 361 nm, $\varepsilon = 2.8 \times 10^4$ M^{-1} cm^{-1}).[48]

Kinetic Measurements. Kinetic measurements for fast reactions with short half-lifetimes were performed on a UNISOKU RSP-601 stopped-flow spectrophotometer with an MOS-type highly selective photodiode array at 298 K using a Unisoku thermostated cell holder. When stopped-flow measurements were carried out under deaerated or O_2-saturated conditions, a deaerated or O_2-saturated PhCN solution with a stream of argon or O_2 was transferred by means of a glass syringe to a spectrometer cell that was already purged with a stream of argon or O_2. Rate constants of oxidation of ferrocene derivatives by O_2 in the presence of a catalytic amount of Co^{II}(Ch) and an excess amount of $HClO_4$ in PhCN at 298 K were determined by monitoring the appearance of an absorption band due to the corresponding ferrocenium ions (Fc^+, λ_{max} 620 nm, $\varepsilon_{max} = 330$ M^{-1} cm^{-1}; Me_2Fc^+, λ_{max} 650 nm, $\varepsilon_{max} = 290$ M^{-1} cm^{-1}; Me_8Fc^+, λ_{max} 750 nm, $\varepsilon_{max} = 410$ M^{-1} cm^{-1}; $BrFc^+$, λ_{max} 620 nm, $\varepsilon_{max} = 320$ M^{-1} cm^{-1}; Br_2Fc^+, λ_{max} 700 nm, $\varepsilon_{max} = 180$ M^{-1} cm^{-1}).[21] At the wavelengths monitored, spectral overlap was observed with $[Co^{II}(ChH)]^+$ (λ 620 nm (1.6×10^4 M^{-1} cm^{-1}), 650 nm (1.4×10^4 M^{-1} cm^{-1}), 700 nm (7.0×10^3 M^{-1} cm^{-1}), 750 nm (2.0×10^3 M^{-1} cm^{-1})). An air-saturated PhCN solution was used for the catalytic reduction of O_2 by ferrocene derivatives. The concentration of O_2 in an air-saturated PhCN solution (1.7×10^{-3} M) was determined as reported previously.[49] The concentrations of ferrocene derivatives employed for the catalytic reduction of O_2 were much larger than that of O_2, when O_2 is the reaction-limiting reagent in the reaction solution. In contrast, the small amount of a ferrocene derivative for the two-electron reduction of O_2 was employed in an O_2-saturated PhCN solution, where a ferrocene derivative is the reaction-limiting reagent.

Electrochemical Measurements. Cyclic voltammetry (CV) measurements were performed on an ALS 630B electrochemical analyzer, and voltammograms were measured in deaerated PhCN containing 0.10 M $TBAPF_6$ as a supporting electrolyte at room temperature. A conventional three-electrode cell was used with a glassy-carbon working electrode (surface area of 0.3 mm^2) and a platinum wire as the counter electrode. The glassy-carbon working electrode (BAS) was routinely polished with BAS polishing alumina suspension and rinsed with acetone before use. The potentials were measured with respect to the $Ag/AgNO_3$ (1.0×10^{-2} M) reference electrode. All potentials (vs $Ag/AgNO_3$) were converted to values vs SCE by adding 0.29 V.[50] Redox potentials were determined using the relation $E_{1/2} = (E_{pa} + E_{pc})/2$.

EPR Measurements. The EPR spectra were measured on a JEOL X-band EPR spectrometer (JES-ME-LX) using a quartz EPR tube containing a deaerated sample frozen solution at 80 K. The internal diameter of the EPR tube is 4.5 mm, which is small enough to fill the EPR cavity but large enough to obtain good signal-to-noise ratios during the EPR measurements at low temperature (at 80 K). The EPR spectra were measured under nonsaturating microwave power conditions. The amplitude of modulation was chosen to optimize the resolution and the signal-to-noise (S/N) ratio of the observed spectra. The g values were calibrated with a Mn^{2+} marker, and the hyperfine coupling (hfc) constants were determined by computer simulation using Calleo EPR Version 1.2 program coded by Calleo Scientific Software Publishers.

RESULTS AND DISCUSSION

Protonation of Co^{II}(Ch). Protonation of Co^{II}(Ch) was studied by the UV−vis absorption spectral change upon addition of $HClO_4$ to a deaerated PhCN solution of Co^{II}(Ch). The characteristic absorption bands of Co^{II}(Ch) at 424 and 646 nm disappeared by the addition of $HClO_4$, as shown in Figure 1a.

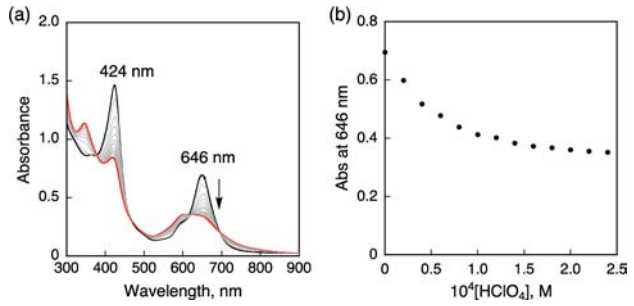

Figure 1. (a) Absorption spectral changes of Co^{II}(Ch) (2.0×10^{-5} M) upon addition of $HClO_4$ in deaerated PhCN at 298 K. (b) Absorbance change at 646 nm upon addition of $HClO_4$.

The change in the absorption spectra can be ascribed to the protonation of Co^{II}(Ch) at the carbonyl group, which is conjugated to the π system of the chlorin ligand to form $[Co^{II}(ChH)]^+$,[43] as shown in Scheme 1.[51]

The protonation induces the decrease of the electron density on the macrocyclic ligand, leading to the low nucleophilicity of the pyrrole nitrogen atoms.[43,52,53] The protonation equilibrium constant of Co^{II}(Ch) with $HClO_4$ (K) was determined by the absorption spectral change at 646 nm to be 2.2×10^4 M^{-1} in deaerated PhCN at 298 K, as shown in Figure1b (eq 1).[47]

$$Co^{II}(Ch) + H^+ \rightleftarrows [Co^{II}(ChH)]^+ \quad (1)$$

dx.doi.org/10.1021/ja312199h | J. Am. Chem. Soc. 2013, 135, 2800−2808

Scheme 1

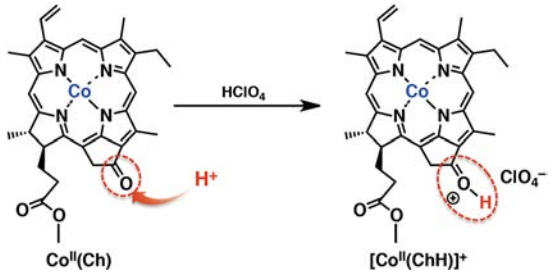

The protonation of $Co^{II}(Ch)$ at the carbonyl group of the chlorin ligand was evidenced by the observation of the EPR spectrum of a deaerated PhCN solution of $Co^{II}(Ch)$ at 80 K (Figure 2). The obtained signal exhibited a well-resolved signals

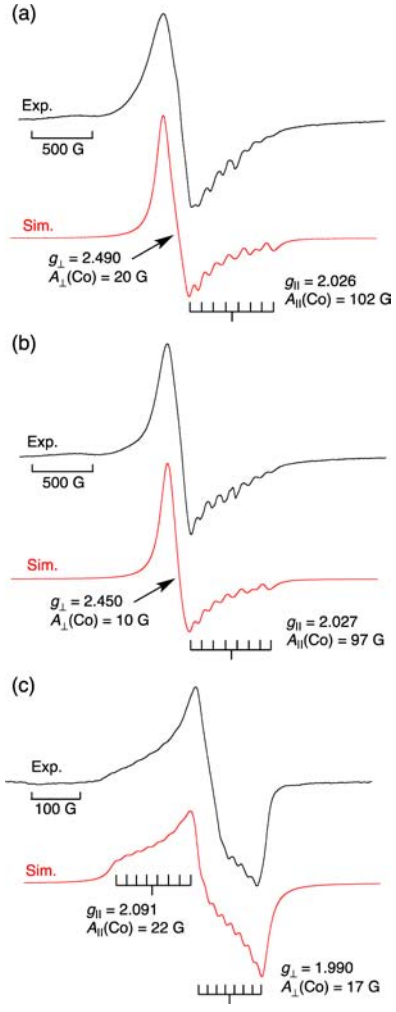

Figure 2. EPR spectra of (a) $Co^{II}(Ch)$ (1.0×10^{-3} M) in deaerated PhCN at 80 K, (b) $Co^{II}(Ch)$ (1.0×10^{-3} M) upon addition of $HClO_4$ (5.0×10^{-3} M) in deaerated PhCN at 80 K, and (c) $Co^{II}(Ch)$ (1.0×10^{-4} M) in air-saturated PhCN at 80 K. The black and red lines show the experimental and simulated spectra, respectively. Experimental parameters: microwave frequency 9.0 GHz, microwave power 1.0 mW, modulation frequency 100 kHz, and modulation width 10 G.

at $g_\perp = 2.490$ and $g_\parallel = 2.026$ with hyperfine splitting due to ^{59}Co ($A_\parallel(^{59}Co) = 102$ G), which are typical for a low-spin ($S = {}^1/_2$) five-coordinate cobalt(II) complex.[21,54] By addition of $HClO_4$ to a deaerated PhCN solution of $Co^{II}(Ch)$ to form $[Co^{II}(ChH)]^+$, only small changes in the EPR parameters were observed, as shown in Figure 2b. The $g_\parallel$ value remained nearly the same, whereas the $g_\perp$ value became slightly smaller on protonation.

The O_2 binding equilibrium of $Co^{II}(Ch)$ was also monitored by the EPR spectral changes. When a PhCN solution of $Co^{II}(Ch)$ is exposed to air, large changes in g values and coupling constant are observed, as shown in Figure 2c, which shows signals at $g_\parallel = 2.091$ and $g_\perp = 1.990$ with hyperfine splitting due to ^{59}Co ($A_\perp(^{59}Co) = 22$ G, $A_\parallel(^{59}Co) = 17$ G). The $g_\parallel$ value is smaller than the reported value for free $O_2^{\bullet-}$ ($g_\parallel = 2.102$), but it is larger than those of $O_2^{\bullet-}$ when it is bound to metal cations and NH_4^+.[55,56] It has been reported that the $g_\parallel$ value of $O_2^{\bullet-}$–metal ion complexes becomes smaller when the interaction between $O_2^{\bullet-}$ and metal ions is increased.[56] However, the observation of superhyperfine due to ^{59}Co (Figure 2c) clearly indicates the existence of an interaction between $O_2^{\bullet-}$ and the Co(III) center. Thus, the observed EPR spectrum in Figure 2c is assigned to the $[Co^{III}(Ch)]^+$–$O_2^{\bullet-}$ complex, in which the interaction between the Co(III) center and $O_2^{\bullet-}$ is relatively weak. The weak binding in the $[Co^{III}(Ch)]^+$–$O_2^{\bullet-}$ complex is confirmed by the reversibility of the formation of the $[Co^{III}(Ch)]^+$–$O_2^{\bullet-}$ complex, which reverts to $Co^{II}(Ch)$ by evacuation of O_2.

The reversible binding of O_2 to $Co^{II}(Ch)$ was also confirmed by the UV–vis absorption spectral change of an air-saturated propionitrile solution of $Co^{II}(Ch)$ at various temperatures. As shown in Figure 3, the absorption bands of $Co^{II}(Ch)$ at 424 and

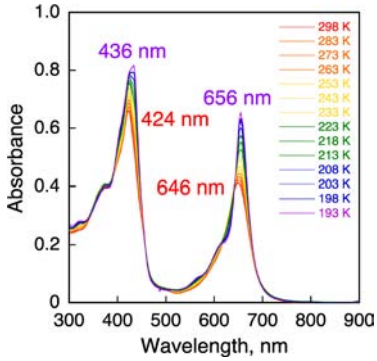

Figure 3. Absorption spectral changes of $Co^{II}(Ch)$ (1.0×10^{-5} M) in air-saturated propionitrile at various temperatures.

646 nm were changed to those at 436 and 656 nm on a decrease in temperature. The changes in the absorption spectra are ascribed due to the O_2 binding of $Co^{II}(Ch)$ to form $[Co^{III}(Ch)]^+$–$O_2^{\bullet-}$ (eq 2).

$$Co^{II}(Ch) + O_2 \rightleftarrows [Co^{III}(Ch)]^+–O_2^{\bullet-} \quad (2)$$

The reversible change between $Co^{II}(Ch)$ and $[Co^{III}(Ch)]^+$–$O_2^{\bullet-}$ was observed by heating or cooling and also by evacuation or introduction of O_2.

The protonation behavior of the one-electron-oxidized species $[Co^{III}(Ch)]^+$ was also monitored by UV–vis titration. $[Co^{III}(Ch)]^+$ was prepared by oxidation of $Co^{II}(Ch)$ by oxygen dissolved in PhCN containing a small amount of $HClO_4$.[19] $[Co^{III}(Ch)]^+$ exhibited a characteristic spectrum with two peak tops at 436 and 656 nm, which is identical with that of $[Co^{III}(Ch)]^+$ prepared by the electron-transfer oxidation of $Co^{II}(Ch)$ by the one-electron-oxidizing reagent (p-$BrC_6H_4)_3N^{\bullet+}SbCl_6^-$ (E_{red} = 1.05 V vs SCE), as shown in Figure S2 (Supporting Information).

dx.doi.org/10.1021/ja312199h | J. Am. Chem. Soc. 2013, 135, 2800–2808

The addition of $HClO_4$ to an air-saturated PhCN solution of $[Co^{III}(Ch)]^+$ showed a spectral change to afford $[Co^{III}(ChH)]^{2+}$, as shown in Figure 4a. In the case of $[Co^{III}(Ch)]^+$, however, a large

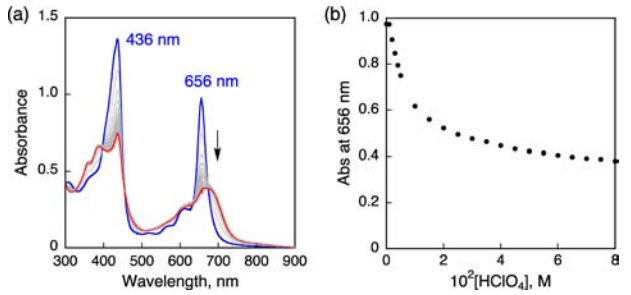

Figure 4. (a) Absorption spectral changes of $[Co^{III}(Ch)]^+$ (1.0×10^{-5} M) upon addition of $HClO_4$ in air-saturated PhCN at 298 K. (b) Absorbance change at 656 nm upon addition of $HClO_4$.

excess of $HClO_4$ was required, in comparison to the case of $Co^{II}(Ch)$, to complete the protonation (Figure 4b). The protonation equilibrium constant of $[Co^{III}(Ch)]^+$ with $HClO_4$ (K) was determined by the absorption spectral change at 656 nm to be 1.1×10^2 M^{-1} in PhCN at 298 K (eq 3).[47]

$$[Co^{III}(Ch)]^+ + H^+ \rightleftarrows [Co^{III}(ChH)]^{2+} \quad (3)$$

The smaller protonation equilibrium constant between $[Co^{III}(Ch)]^+$ and $[Co^{III}(ChH)]^{2+}$ results from a small electron density on the chlorin ligand. This is caused by the electronic interaction between the high-valent Co(III) ion and the lone pairs of the nitrogen atoms on chlorin ligand.[52,53]

Electrochemical measurements on $Co^{II}(Ch)$ and $Co^{II}(OEP)$ were performed in deaerated PhCN containing 0.10 M $TBAPF_6$ to determine the catalytic activity of cobalt complexes toward the reduction of O_2, as shown in Figure 5. In the case of $Co^{II}(Ch)$,

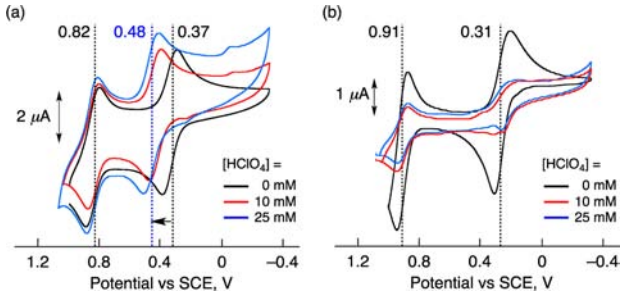

Figure 5. Cyclic voltammograms of deaerated PhCN solutions of (a) $Co^{II}(Ch)$ (1.0×10^{-3} M) recorded in the presence of $TBAPF_6$ (0.10 M) without $HClO_4$ (black line), with $HClO_4$ (1.0×10^{-2} M) (red line), and with $HClO_4$ (2.5×10^{-2} M) (blue line) and (b) $Co^{II}(OEP)$ (1.0×10^{-3} M) recorded in the presence of $TBAPF_6$ (0.10 M) without $HClO_4$ (black line), with $HClO_4$ (1.0×10^{-2} M) (red line), and with $HClO_4$ (2.5×10^{-2} M) (blue line). The sweep rate was 100 mV s^{-1}.

the reversible redox couples $[Co^{III}(Ch)]^+/Co^{II}(Ch)$ and $[Co^{III}(Ch^{\bullet+})]^{2+}/[Co^{III}(Ch)]^+$ were observed at $E_{1/2}$ = 0.37, 0.82 V (vs SCE),[14] respectively, as shown in Figure 5a (black). In the presence of $HClO_4$ (Figure 5a, blue), the redox wave for $[Co^{III}(Ch^{\bullet+})]^{2+}/[Co^{III}(Ch)]^+$ was observed at 0.82 V, which is the virtually the same as that in the absence of $HClO_4$, whereas the redox potential for $[Co^{III}(Ch)]^+/Co^{II}(Ch)$ was positively shifted from $E_{1/2}$ = 0.37 to 0.48 V (vs SCE). This is consistent with chlorin ligand protonation, which causes the positive shift of the center-metal redox potential due to a decrease in the electron density of the chlorin ligand,[52,53] as described above.

When $Co^{II}(Ch)$ is replaced by a cobalt(II) porphyrin ($Co^{II}(OEP)$; OEP = octaethylporphyrin), the reversible couples $[Co^{III}(OEP)]^+/Co^{II}(OEP)$ and $[Co^{III}(OEP^{\bullet+})]^{2+}/[Co^{III}(OEP)]^+$ similar to those of $Co^{II}(Ch)$ were observed at $E_{1/2}$ = 0.31, 0.91 V (vs SCE),[14] respectively, as shown in Figure 5b (black). In contrast to the case for $Co^{II}(Ch)$, the addition of $HClO_4$ to a deaerated PhCN solution of $Co^{II}(OEP)$ resulted in a decrease in current due to demetalation of the center-metal ion from the macrocyclic ligand (blue line in Figure 5b) (vide infra). The oxidation peak for demetalated $Co^{II}(OEP)$ by $HClO_4$ ($[H_4(OEP)]^{2+}$) was observed at 1.5 V vs SCE in the CV measurement of $Co^{II}(OEP)$ with $HClO_4$ (Figure S3a, Supporting Information). This value agrees with the one-electron oxidation peak of $[H_4(OEP)]^{2+}$ (Figure S3b, Supporting Information).

When $Co^{II}(Ch)$ is employed as a catalyst for the electrochemical reduction of O_2 in O_2-saturated PhCN containing 0.10 M $TBAPF_6$, catalytic currents corresponding to the reduction of O_2 with an onset potential of 0.6 V (vs SCE) were observed, as shown in Figure 6a. The onset potential for the reduction of O_2 with $Co^{II}(Ch)$ is more positive than in the case of $Co^{II}(OEP)$ (Figure 6).

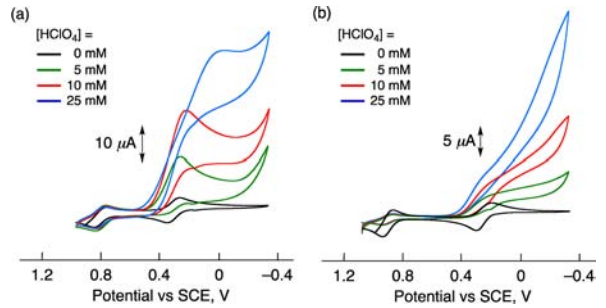

Figure 6. Cyclic voltammograms of O_2-saturated PhCN solutions of (a) $Co^{II}(Ch)$ (1.0×10^{-3} M) recorded in the presence of 0.10 M $TBAPF_6$ without $HClO_4$ (black line), with $HClO_4$ (5.0×10^{-3} M) (green line), with $HClO_4$ (1.0×10^{-2} M) (red line), and with $HClO_4$ (2.5×10^{-2} M) (blue line) and (b) $Co^{II}(OEP)$ (1.0×10^{-3} M) recorded in the presence of 0.10 M $TBAPF_6$ without $HClO_4$ (black line), with $HClO_4$ (5.0×10^{-3} M) (green line), with $HClO_4$ (1.0×10^{-2} M) (red line), and with $HClO_4$ (2.5×10^{-2} M) (blue line). The sweep rate was 10 mV s^{-1}.

As far as we know, this value of onset potential for the two-electron reduction of O_2 is the largest (the least overpotential), in comparison to those of other metal complexes for the two-electron reduction of O_2.[4,13]

Catalytic Two-Electron Reduction of O_2 by Me_2Fc with $Co^{II}(Ch)$ in the Presence of $HClO_4$. The addition of $HClO_4$ to an air-saturated PhCN solution of $Co^{II}(Ch)$ and 1,1′-dimethylferrocene (Me_2Fc) resulted in the efficient oxidation of Me_2Fc by O_2 to produce 1,1′-dimethylferrocenium ion (Me_2Fc^+). It should be noted that no oxidation of Me_2Fc occurred by O_2 in the absence of $Co^{II}(Ch)$ under the present acidic conditions. The stoichiometry of the catalytic oxygen reduction was confirmed under the reaction conditions using air-saturated O_2 (concentration 1.7×10^{-3} M) in PhCN. The formation of Me_2Fc^+ was monitored by a rise in absorbance at 650 nm, as shown in Figure 7a. The rising curved line in Figure 7b shows the time course of the formation of Me_2Fc^+ in the reduction of O_2 (1.7×10^{-3} M) in the presence of a catalytic

dx.doi.org/10.1021/ja312199h | J. Am. Chem. Soc. 2013, 135, 2800−2808

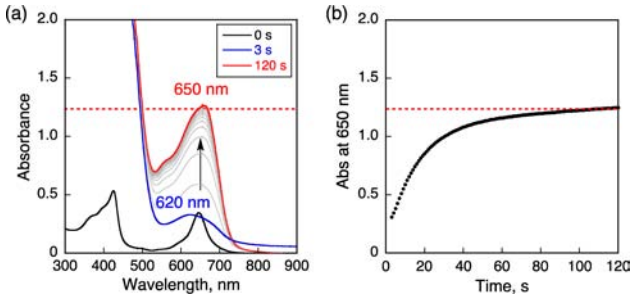

Figure 7. (a) Absorption spectral changes in the two-electron reduction of O_2 (1.7×10^{-3} M) by Me_2Fc (2.5×10^{-2} M) with $Co^{II}(Ch)$ (1.0×10^{-5} M) in the presence of $HClO_4$ (2.5×10^{-2} M) in air-saturated PhCN at 298 K. The black and red lines show the spectra before and after addition of $HClO_4$, respectively. The blue line shows the spectrum of the intermediate in the catalytic reaction. The dotted line is the absorbance at 650 nm due to 3.4×10^{-3} M Me_2Fc^+. (b) Time profile of absorbance at 650 nm due to Me_2Fc^+.

amount of $Co^{II}(Ch)$ (1.0×10^{-5} M), a large excess of Me_2Fc (2.5×10^{-2} M) and $HClO_4$ (2.5×10^{-2} M). At the end of the catalytic reaction, the concentration of Me_2Fc^+ (3.4×10^{-3} M) formed in the catalytic reduction of O_2 by Me_2Fc is twice the concentration of O_2 (1.7×10^{-3} M) in air-saturated PhCN. This result clearly indicates that the two-electron reduction of O_2 occurs to produce 2 equiv of Me_2Fc^+ and there is no further reduction to produce more than 2 equiv of Me_2Fc^+, which is in agreement with results for other mononuclear Co(II) complexes (eq 4).[11,19,21]

The stoichiometric production of H_2O_2 was ascertained by performing the iodometric titration,[48] which is the reaction of an

$$O_2 + 2H^+ + 2Me_2Fc \xrightarrow[Co^{II}(Ch)]{} H_2O_2 + 2Me_2Fc^+ \quad (4)$$

excess amount of NaI in deaerated CH_3CN (2.0 mL) with the 50 times diluted reaction mixture of $Co^{II}(Ch)$ (2.0×10^{-7} M), Me_2Fc^+ (6.8×10^{-5} M), and $HClO_4$ (5.0×10^{-4} M) (Figure S4, Supporting Information). The catalytic turnover number (TON = mol of H_2O_2 as the product of the two-electron reduction of O_2/mol of $Co^{II}(Ch)$) was determined from the concentration of Me_2Fc^+ to be more than 30000, when the concentrations of $Co^{II}(Ch)$, Me_2Fc, and $HClO_4$ in O_2-saturated PhCN were 2.0×10^{-7}, 2.5×10^{-2}, and 2.5×10^{-2} M, respectively.

The intermediate observed during the catalytic reaction shown by the broad blue line around 620 nm in Figure 7a was identified as $[Co^{II}(ChH)]^+$ by comparison with the absorption spectrum of $[Co^{II}(ChH)]^+$ produced by the addition of $HClO_4$ to a deaerated PhCN solution of $Co^{II}(Ch)$ in Figure 1. This suggests that proton-coupled electron transfer (PCET) from $[Co^{II}(ChH)]^+$ to O_2 is the rate-determining step under the catalytic conditions (vide infra).

When $Co^{II}(OEP)$ was employed as a catalyst under the same catalytic conditions as the case of $Co^{II}(Ch)$, $Co^{II}(OEP)$ was oxidized by O_2 to form $[Co^{III}(OEP)]^+$ as soon as the two-electron reduction of O_2 was initiated (Figure S5, Supporting Information).[19] During the catalytic two-electron reduction of O_2, the absorption bands associated with $[Co^{III}(OEP)]^+$ decreased rapidly, accompanied by an increase of new absorption bands due to $[H_4(OEP)]^{2+}$ formed by demetalation and diprotonation, as shown in Scheme 2 (Figures S6 and S7, Supporting Information). These results indicate that fast demetalation of $Co^{II}(OEP)$ occurred, followed by the protonation of $H_2(OEP)$ to form $[H_4(OEP)]^{2+}$ (vide supra).

Scheme 2

Kinetics and Mechanism of Two-Electron Reduction of O_2 by Me_2Fc with $Co^{II}(Ch)$. The catalytic rate constant (k_{cat}) was determined from the dependence of the observed rate constant (k_{obs}) for formation of Me_2Fc^+ on the concentrations of $Co^{II}(Ch)$, $HClO_4$, Me_2Fc, and O_2 (Figure 8). The k_{obs} value was

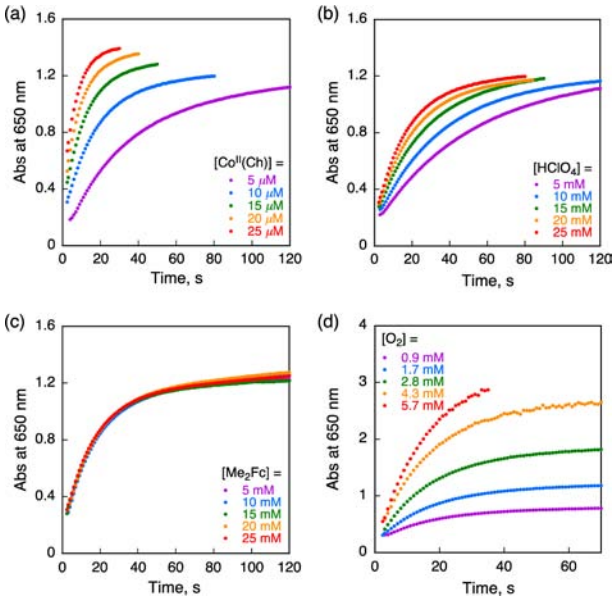

Figure 8. (a) Time profiles of absorbance at 650 nm due to Me_2Fc^+ in the two-electron reduction of O_2 (1.7×10^{-3} M) by Me_2Fc (2.5×10^{-2} M) with various concentrations of $Co^{II}(Ch)$ in the presence of $HClO_4$ (2.5×10^{-2} M) in air-saturated PhCN at 298 K. (b) Time profiles of absorbance at 650 nm due to Me_2Fc^+ in the two-electron reduction of O_2 (1.7×10^{-3} M) by Me_2Fc (2.5×10^{-2} M) with $Co^{II}(Ch)$ (1.0×10^{-5} M) in the presence of various concentrations of $HClO_4$ in PhCN at 298 K. (c) Time profiles of absorbance at 650 nm due to Me_2Fc^+ in the two-electron reduction of O_2 (1.7×10^{-3} M) by various concentrations of Me_2Fc with $Co^{II}(Ch)$ (1.0×10^{-5} M) in the presence of $HClO_4$ (2.5×10^{-2} M) in PhCN at 298 K. (d) Time profiles of absorbance at 650 nm due to Me_2Fc^+ in the two-electron reduction of various concentrations of O_2 by Me_2Fc (2.5×10^{-2} M) with $Co^{II}(Ch)$ (1.0×10^{-5} M) in the presence of $HClO_4$ (2.5×10^{-2} M) in PhCN at 298 K.

determined from the increase in absorbance at 650 nm, obeying pseudo-first-order kinetics under the reaction conditions limited by air-saturated O_2 concentration in PhCN (Figure S8, Supporting Information).[57] This indicates that the reduction of O_2 is involved in the rate-determining step.

The pseudo-first-order rate constant (k_{obs}) is proportional to the concentration of $Co^{II}(Ch)$ without intercept (Figure 9a). The k_{obs} values increased linearly with increasing concentration of $HClO_4$ with an intercept (Figure 9b), whereas the k_{obs} values remained constant irrespective of the concentrations of Me_2Fc (Figure 9c) or O_2 (Figure 9d). The observed first-order kinetics

dx.doi.org/10.1021/ja312199h | J. Am. Chem. Soc. 2013, 135, 2800−2808

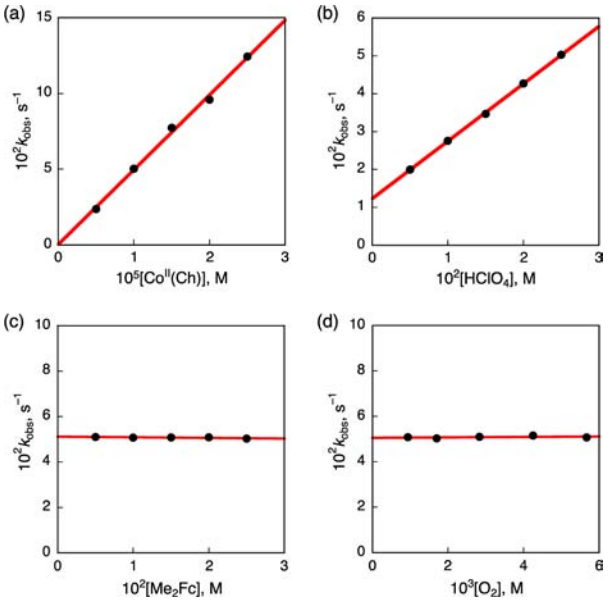

Figure 9. (a) Plot of k_{obs} vs [Co^{II}(Ch)] for the two-electron reduction of O_2 (1.7×10^{-3} M) by Me_2Fc (2.5×10^{-2} M) in the presence of $HClO_4$ (2.5×10^{-2} M) in air-saturated PhCN. (b) Plot of k_{obs} vs [$HClO_4$] for the two-electron reduction of O_2 (1.7×10^{-3} M) by Me_2Fc (2.5×10^{-2} M) with Co^{II}(Ch) (1.0×10^{-5} M) in the presence of various concentrations of $HClO_4$ in PhCN at 298 K. (c) Plot of k_{obs} vs [Me_2Fc] for the two-electron reduction of O_2 (1.7×10^{-3} M) by various concentrations of Me_2Fc with Co^{II}(Ch) (1.0×10^{-5} M) in the presence of $HClO_4$ (2.5×10^{-2} M) in PhCN at 298 K. (d) Plot of k_{obs} vs [O_2] for the two-electron reduction of various concentrations of O_2 by Me_2Fc (2.5×10^{-2} M) with Co^{II}(Ch) (1.0×10^{-5} M) in the presence of $HClO_4$ (2.5×10^{-2} M) in PhCN at 298 K.

depending on the concentrations of Co^{II}(Ch), $HClO_4$, and O_2 indicates that proton-coupled electron transfer (PCET) from [Co^{II}(ChH)]$^+$ to O_2 to produce [Co^{III}(ChH)]$^{2+}$ and $HO_2^\bullet$ is the rate-determining step in the catalytic cycle, as shown in Scheme 3.

Scheme 3

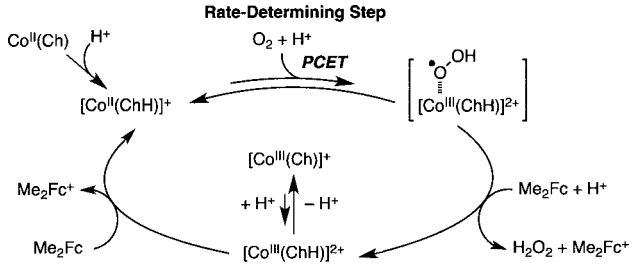

The produced $HO_2^\bullet$ is rapidly reduced by Me_2Fc with H^+ to produce H_2O_2. The PCET process as the rate-determining step is also supported by the steady-state appearance of [Co^{II}(ChH)]$^+$ as the intermediate in the catalytic cycle (vide supra). On the other hand, [Co^{III}(ChH)]$^{2+}$, which is in the protonation equilibrium with [Co^{III}(Ch)]$^+$, as shown in Figure 4, is also rapidly reduced by Me_2Fc to regenerate [Co^{II}(ChH)]$^+$. Thus, the kinetic equation is given by eq 5, where the $k_{cat(1)}$ value was determined from the intercept of the linear plot of k_{obs} vs [$HClO_4$] to be $(1.2 \pm 0.2) \times 10^3$ M^{-1} s^{-1} (Figure 9b). The observation of the intercept indicates that proton-coupled electron transfer from [Co^{II}(ChH)]$^+$ to O_2 proceeds even in the absence of excess $HClO_4$. The $k_{cat(2)}$ value was determined from the slopes of the linear plot of k_{obs} vs [Co^{II}(Ch)] and [$HClO_4$] to be $(1.9 \pm 0.3) \times 10^5$ M^{-2} s^{-1} (Figure 9a,b, respectively).

$$d[Me_2Fc^+]/dt = (k_{cat(1)} + k_{cat(2)}[HClO_4])[[Co^{II}(ChH)]^+][O_2] \quad (5)$$

The kinetic equation (eq 5) was also confirmed under reaction conditions where the concentrations of O_2 were in large excess to Me_2Fc (Figure 10). In such a case, the concentration of a large

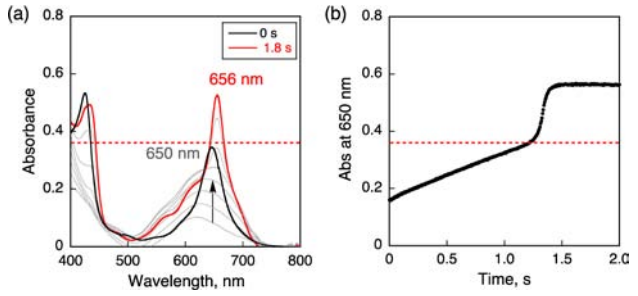

Figure 10. (a) Absorption spectral changes in the two-electron reduction of O_2 (8.5×10^{-3} M) by Me_2Fc (6.5×10^{-4} M) with Co^{II}(Ch) (1.0×10^{-5} M) in the presence of $HClO_4$ (5.0×10^{-2} M) in O_2-saturated PhCN at 298 K. The black and red lines show the spectra before and after addition of $HClO_4$, respectively. The dotted line is the absorbance at 650 nm due to 6.5×10^{-4} M Me_2Fc^+. (b) Time profile of absorbance at 650 nm due to Me_2Fc^+.

excess of O_2 remained constant during the catalytic reduction of O_2 by Me_2Fc, where the rate of formation of Me_2Fc^+ exhibited zero-order kinetics, as shown in Figure 10b. When the catalytic reaction was complete, a steep rise in absorbance at 650 nm due to [Co^{III}(ChH)]$^{2+}$ was observed at around 1.3 s (Figure 10b), because Me_2Fc was consumed not to reduce [Co^{III}(ChH)]$^{2+}$. This result suggests that the catalytic reduction of O_2 with Co^{II}(Ch) proceeds efficiently without decomposition of the catalyst because of its high durability under the acidic conditions, in contrast with the case of Co(OEP). The pseudo-zero-order rate constant ($k_{obs(0)}$) was proportional to concentration of Co^{II}(Ch) (Figure S9a, Supporting Information). The $k_{obs(0)}$ values increased linearly with increasing concentration of $HClO_4$ with an intercept (Figure S9b, Supporting Information), whereas the $k_{obs(0)}$ values remained constant irrespective of the concentration of Me_2Fc (Figure S9c, Supporting Information). These results are totally consistent with the kinetic formation in eq 5. In order to further confirm the catalytic mechanism in Scheme 3, each step in the catalytic cycle was examined separately (vide infra).

PCET from [Co^{II}(ChH)]$^+$ to O_2. As described above, Co^{II}(Ch) reacts with O_2 reversibly to produce [Co^{III}(Ch)]$^+$–$O_2^{\bullet-}$ (eq 2) at low temperature. At 298 K the equilibrium lies largely to the Co^{II}(Ch) side when no appreciable oxidation of Co^{II}Ch by O_2 was observed. The addition of $HClO_4$ to an air-saturated PhCN solution of Co^{II}(Ch), however, resulted in rapid PCET from [Co^{II}(ChH)]$^+$ to O_2 to afford [Co^{III}(ChH)]$^{2+}$, as shown in Figure 11a. The rate of formation of [Co^{III}(ChH)]$^{2+}$ was determined from the rise in absorbance at 656 nm due to [Co^{III}(ChH)]$^{2+}$, obeying first-order kinetics. The pseudo-first-order-rate constant (k_{obs}) increased linearly with increasing concentration of $HClO_4$ with an intercept as shown in Figure 11b. In this case, the kinetic equation is given by eq 6. From the intercept of the linear plot of k_{obs} vs [$HClO_4$], the second-order rate constant $k_{(1)}$,

$$d[[Co^{III}(ChH)]^{2+}]/dt = (k_1 + k_2[HClO_4])[[Co^{II}(ChH)]^+][O_2] \quad (6)$$

dx.doi.org/10.1021/ja312199h | J. Am. Chem. Soc. 2013, 135, 2800−2808

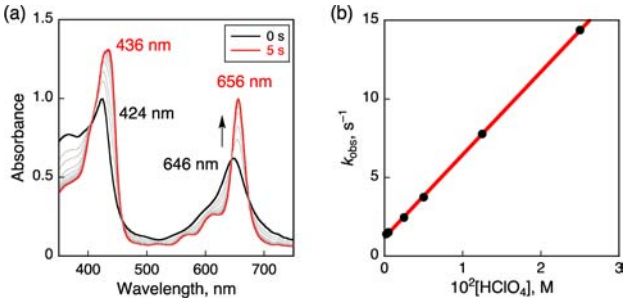

Figure 11. (a) Absorption spectral changes in the two-electron reduction of O_2 (1.7×10^{-3} M) with $Co^{II}(Ch)$ (2.0×10^{-5} M) in the presence of various concentrations of $HClO_4$ in air-saturated PhCN at 298 K. (b) Plot of k_{obs} vs [$HClO_4$].

which is independent of the concentration of [$HClO_4$], was determined to be $(1.0 \pm 0.3) \times 10^3$ M^{-1} s^{-1}.

On the other hand, the third-order rate constant $k_{(2)}$ was determined from the slope to be $(2.1 \pm 0.2) \times 10^5$ M^{-2} s^{-1}. The $k_{(1)}$ and $k_{(2)}$ values agreed within experimental errors with the rate constants derived under catalytic conditions ($k_{cat(1)} = (1.2 \pm 0.2) \times 10^3$ M^{-1} s^{-1} and $k_{cat(2)} = (1.9 \pm 0.3) \times 10^5$ M^{-2} s^{-1}, respectively). Such agreements confirm that the rate-determining step in the catalytic cycle in Scheme 3 is indeed the PCET from $[Co^{II}(ChH)]^+$ to O_2.

Reduction of $[Co^{III}(ChH)]^{2+}$. The aforementioned results indicate that the electron-transfer reduction of $[Co^{III}(ChH)]^{2+}$ by Me_2Fc is much faster than the PCET oxidation of $[Co^{II}(ChH)]^+$. This was independently confirmed by examining electron transfer from Me_2Fc to $[Co^{III}(Ch)]^+$, which was prepared by the oxidation of $Co^{II}(Ch)$ with $(p\text{-}BrC_6H_4)_3N^{\bullet+}SbCl_6^-$ as a one-electron oxidant, as shown in Figure 12a.

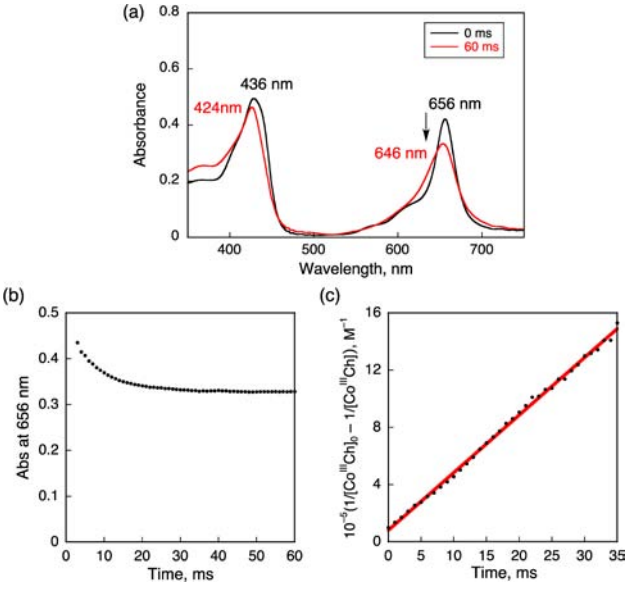

Figure 12. (a) Absorption spectral changes in the electron-transfer reduction of $[Co^{III}(Ch)]^+$ (1.0×10^{-5} M) with Me_2Fc (1.0×10^{-5} M) in deaerated PhCN at 298 K. (b) Time profile monitored by absorbance (Abs) at 656 nm. (c) Second-order plot.

The rate of the reduction of $[Co^{III}(Ch)]^+$ by 1 equiv of Me_2Fc was determined from a decrease in absorbance at 656 nm due to $[Co^{III}(Ch)]^+$ using a stopped-flow technique (Figure 12b). The second-order rate constant was determined from the second-order plot to be $(4.0 \pm 0.3) \times 10^7$ M^{-1} s^{-1} (Figure 12c). It is noted that the electron-transfer reduction of $[Co^{III}(ChH)]^{2+}$ (E_{red} = 0.48 V vs SCE) by Me_2Fc should be faster than the electron-transfer reduction of $[Co^{III}(Ch)]^+$ (E_{red} = 0.37 V vs SCE) by Me_2Fc. This result confirmed that the electron-transfer reduction of $[Co^{III}(ChH)]^{2+}$ by Me_2Fc was much faster than the PCET reduction of O_2 by $[Co^{II}(ChH)]^+$.

Because electron transfer from Me_2Fc to $[Co^{III}(ChH)]^{2+}$ is fast enough not to be the rate-determining step, the replacement of Me_2Fc by a stronger one-electron reductant would give the same catalytic rate constant. This was confirmed by using octamethylferrocene (Me_8Fc: E_{ox} = −0.04 V vs SCE) for the catalytic two-electron reduction of O_2 (1.7×10^{-3} M) with $Co^{II}(Ch)$ in the presence of $HClO_4$ (2.5×10^{-2} M) in PhCN. The observed first-order rate constant remained the same irrespective of concentration of Me_8Fc to be $(4.3 \pm 0.3) \times 10^{-2}$ s^{-1} (Figure S10a, Supporting Information), which is about the same as the value for Me_2Fc $(5.0 \pm 0.3) \times 10^{-2}$ s^{-1} (Figure 9c). When Me_2Fc (E_{ox} = 0.28 V) was replaced by weaker one-electron reductants, ferrocene (Fc: E_{ox} = 0.37 V) and bromoferrocene (BrFc: E_{ox} = 0.54 V), the observed first-order rate constants also remained the same as those for Me_2Fc and Me_8Fc irrespective of concentrations of Fc and BrFc, as shown in Figure S10b,c (Supporting Information), respectively. This suggests that electron transfer from BrFc to $[Co^{III}(ChH)]^{2+}$ is not the rate-determining step in the catalytic cycle, although electron transfer from BrFc to $[Co^{III}(ChH)]^{2+}$ (E_{red} = 0.48 V) is slightly endergonic, as shown in Scheme 4.

Scheme 4

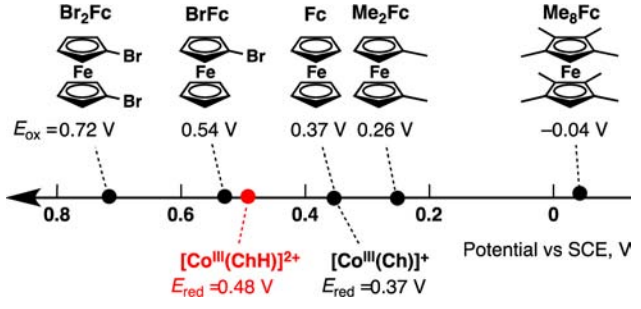

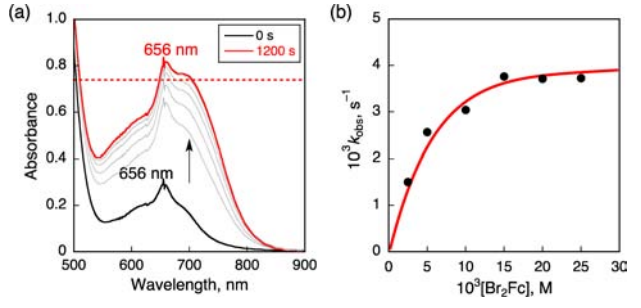

Figure 13. (a) Absorption spectral change in the two-electron reduction of O_2 (1.7×10^{-3} M) by Br_2Fc (2.0×10^{-2} M) with $Co^{II}(Ch)$ (1.0×10^{-5} M) in the presence of $HClO_4$ (2.5×10^{-2} M) in air-saturated PhCN at 298 K. The black and red lines show the spectra before and after addition of Br_2Fc, respectively. The dotted line is the absorbance at 700 nm due to 3.4×10^{-3} M Br_2Fc^+. (b) Plot of k_{obs} vs [Br_2Fc] for the two-electron reduction of O_2 (1.7×10^{-3} M) by Br_2Fc with $Co^{II}(Ch)$ (1.0×10^{-5} M) in the presence of $HClO_4$ (2.5×10^{-2} M) in PhCN at 298 K.

dx.doi.org/10.1021/ja312199h | J. Am. Chem. Soc. 2013, 135, 2800−2808

When 1,1′-dibromoferrocene (Br_2Fc: E_{ox} = 0.72 V) was employed as a weaker reductant than BrFc (Scheme 4), the efficient catalytic two-electron reduction of O_2 still occurred, as shown in Figure 13a, where the absorption band due to $[Co^{III}(ChH)]^{2+}$ (λ_{max} 656 nm) was observed during the catalytic reaction. The rate of formation of Br_2Fc^+ became much slower than those of other stronger one-electron reductants (e.g., Fc) and the observed first-order constants increased with increasing concentration of Br_2Fc, as shown in Figure 13b. This indicates that the rate-determining step is now changed from the PCET reduction of O_2 to the ET reduction of $[Co^{III}(ChH)]^{2+}$ because electron transfer from Br_2Fc to $[Co^{III}(ChH)]^{2+}$ becomes thermodynamically more unfavorable (Scheme 4). At large concentrations of Br_2Fc, however, the rate exhibits a saturation behavior (Figure 13b).[58]

CONCLUSION

We have demonstrated that a cobalt chlorin complex ($Co^{II}(Ch)$) efficiently catalyzes selective two-electron reduction of O_2 by one-electron reductants in the presence of $HClO_4$ in PhCN to produce H_2O_2 with high catalyst stability, where the TON reached more than 30000. This remarkable stability can be explained by two features of the chlorin ligand. One is the larger core size and greater flexibility of the ligand. The other is the lower nucleophilicity of the core nitrogen atoms due to the protonation of the ligand at the carbonyl group (position C-13[1]) in the presence of $HClO_4$. When $Co^{II}(Ch)$ is employed as a catalyst for an electrochemical reduction of O_2, catalytic currents correspond to the two-electron reduction of O_2 with the highest onset potential being 0.6 V (vs SCE). Such a positive onset potential is induced by the protonation of the ligand, where the one-electron-reduction potential of $[Co^{III}(ChH)]^{2+}$ is positively shifted from 0.37 V (vs SCE) to 0.48 V upon addition of $HClO_4$. A detailed kinetic study has revealed the mechanism of the catalytic two-electron reduction of O_2, where the rate-determining step is proton-coupled electron transfer (PCET) from $[Co^{II}(ChH)]^{+}$ to O_2 rather than ET from one-electron reductants to $[Co^{III}(ChH)]^{2+}$. When Br_2Fc is employed as a much weaker reductant than other ferrocene derivatives under the catalytic conditions, the rate-determining step is changed to the ET reduction of $[Co^{III}(ChH)]^{2+}$. In summary, the present study provides valuable insights toward the development of more efficient catalysts for the selective two-electron reduction of O_2 to produce H_2O_2, which is a promising candidate for a renewable energy source.

ASSOCIATED CONTENT

Supporting Information

Text and figures giving spectroscopic and kinetic data. This material is available free of charge via the Internet at http://pubs.acs.org.

AUTHOR INFORMATION

Corresponding Author

*E-mail: fukuzumi@chem.eng.osaka-u.ac.jp.

Notes

The authors declare no competing financial interest.

ACKNOWLEDGMENTS

This work was supported by Grants-in-Aid (Nos. 20108010 to S.F. and 23750014 to K.O.) from MEXT, Japan, and KOSEF/MEST through WCU project (R31-2008-000-10010-0), Korea.

REFERENCES

(1) (a) Abrantes, S.; Amaral, E.; Costa, A. P.; Shatalov, A. A.; Duarte, A. P. *Ind. Crop. Prod.* **2007**, *25*, 288. (b) Zeronian, S. H.; Inglesby, M. K. *Cellulose* **1995**, *2*, 265.

(2) Li, L.; Lee, S.; Lee, H. L.; Youn, H. J. *BioResources* **2011**, *6*, 721.

(3) (a) Disselkamp, R. S. *Energy Fuels* **2008**, *22*, 2771. (b) Disselkamp, R. S. *Int. J. Hydrogen Energy* **2010**, *35*, 1049.

(4) Yamada, Y.; Fukunishi, Y.; Yamazaki, S.; Fukuzumi, S. *Chem. Commun.* **2010**, *46*, 7334.

(5) Yamazaki, S.; Siroma, Z.; Senoh, H.; Ioroi, T.; Fujiwara, N.; Yasuda, K. *J. Power Sources* **2008**, *178*, 20.

(6) (a) Fukuzumi, S.; Yamada, Y.; Karlin, K. D. *Electrochim. Acta* **2012**, *82*, 493. (b) Yamada, Y.; Yoshida, S.; Honda, T.; Fukuzumi, S. *Energy Environ. Sci.* **2011**, *4*, 2822. (c) Jing, X.; Cao, D.; Liu, Y.; Wang, G.; Yin, J.; Wen, Q.; Gao, Y. *J. Electroanal. Chem.* **2011**, *658*, 46.

(7) Sanli, A. E.; Aytaç, A. *Int. J. Hydrogen Energy* **2011**, *36*, 869.

(8) Shaegh, S. A. M.; Nguyen, N.-T.; Ehteshami, S. M. M.; Chan, S. H. *Energy Environ. Sci.* **2012**, *5*, 8225.

(9) For metal−hydrogen peroxide semifuel cells, see: (a) Lei, T.; Tian, Y. M.; Wang, G. L.; Yin, J. L.; Gao, Y. Y.; Wen, Q.; Cao, D. X. *Fuel Cells* **2011**, *11*, 431. (b) Hasvold, O.; Storkersen, N.; Forseth, S.; Lian, T. *J. Power Sources* **2006**, *162*, 935. (c) Patrissi, C. J.; Bessette, R. R.; Kim, Y. K.; Schumacher, C. R. *J. Electrochem. Soc.* **2008**, *155*, B558.

(10) Santacesaria, E.; Serio, M. D.; Velotti, R.; Leone, U. *Ind. Eng. Chem. Res.* **1994**, *33*, 277.

(11) Zagal, J. H.; Griveau, S.; Silva, J. F.; Nyokong, T.; Bedioui, F. *Coord. Chem. Rev.* **2010**, *254*, 2755.

(12) Collman, J. P.; Boulatov, R.; Sunderland, C. J. In *The Porphyrin Handbook*; Kadish, K. M., Smith, K. M., Guilard, R., Eds.; Academic Press: San Diego, CA, 2003; Vol. *11*, p 1.

(13) (a) Kadish, K. M.; Frémond, L.; Shen, J.; Chen, P.; Ohkubo, K.; Fukuzumi, S.; El Ojaimi, M.; Gros, C. P.; Barbe, J.-M.; Guilard, R. *Inorg. Chem.* **2009**, *48*, 2571. (b) Chen, P.; Lau, H.; Habermeyer, B.; Gros, C. P.; Barbe, J.-M.; Kadish, K. M. *J. Porphyrins Phthalocyanines* **2012**, *16*, 762.

(14) (a) Kadish, K. M.; Frémond, L.; Ou, Z.; Shao, J.; Shi, C.; Anson, F. C.; Burdet, F.; Gros, C. P.; Guilard, R. *J. Am. Chem. Soc.* **2005**, *127*, 5625. (b) Kadish, K. M.; Shen, J.; Frémond, L.; Chen, P.; El Ojaimi, M.; Chkounda, M.; Gros, C. P.; Barbe, J.-M.; Ohkubo, K.; Fukuzumi, S.; Guilard, R. *Inorg. Chem.* **2008**, *47*, 6726.

(15) (a) Partovi-Nia, R.; Su, B.; Méndez, M. A; Habermeyer, B.; Gros, C. P.; Barbe, J.-M.; Samec, Z.; Girault, H. H. *ChemPhysChem* **2010**, *11*, 2979. (b) Su, B.; Hatay, I.; Trojánek, A.; Samec, Z.; Khoury, T.; Gros, C. P.; Barbe, J.-M.; Daina, A.; Carrupt, P.-A.; Girault, H. H. *J. Am. Chem. Soc.* **2010**, *132*, 2655.

(16) (a) Anson, F. C.; Shi, C.; Steiger, B. *Acc. Chem. Res.* **1997**, *30*, 437. (b) Shi, C.; Steiger, B.; Yuasa, M.; Anson, F. C. *Inorg. Chem.* **1997**, *36*, 4294. (c) Shi, C.; Anson, F. C. *Inorg. Chem.* **1998**, *37*, 1037. (d) Liu, Z.; Anson, F. C. *Inorg. Chem.* **2000**, *39*, 274.

(17) Yamanaka, I.; Tazawa, S.; Murayama, T.; Ichihashi, R.; Hanaizumi, N. *ChemPhysChem* **2008**, *1*, 988.

(18) Fellinger, T.-P.; Hasche, F.; Strasser, P.; Antonietti, M. *J. Am. Chem. Soc.* **2012**, *134*, 4072.

(19) (a) Fukuzumi, S.; Okamoto, K.; Gros, C. P.; Guilard, R. *J. Am. Chem. Soc.* **2004**, *126*, 10441. (b) Fukuzumi, S.; Okamoto, K.; Tokuda, Y.; Gros, C. P.; Guilard, R. *J. Am. Chem. Soc.* **2004**, *126*, 17059. (c) Fukuzumi, S. *Chem. Lett.* **2008**, *37*, 808. (d) Fukuzumi, S.; Mochizuki, S.; Tanaka, T. *Inorg. Chem.* **1989**, *28*, 2459. (e) Fukuzumi, S.; Mochizuki, S.; Tanaka, T. *Inorg. Chem.* **1990**, *29*, 653. (f) Fukuzumi, S.; Mochizuki, S.; Tanaka, T. *J. Chem. Soc., Chem. Commun.* **1989**, 391.

(20) Fukuzumi, S.; Mandal, S.; Mase, K.; Ohkubo, K.; Park, H.; Benet-Buchholz, J.; Nam, W.; Llobet, A. *J. Am. Chem. Soc.* **2012**, *134*, 9906.

(21) Honda, T.; Kojima, T.; Fukuzumi, S. *J. Am. Chem. Soc.* **2012**, *134*, 4196.

(22) (a) Chang, C. J.; Deng, Y.; Shi, C.; Anson, F. C.; Nocera, D. G. *Chem. Commun.* **2010**, *46*, 7334. (b) Chang, C. J.; Loh, Z.-H.; Shi, C.; Anson, F. C.; Nocera, D. G. *J. Am. Chem. Soc.* **2004**, *126*, 10013. (c) McGuire, R.; Dogutan, D. K.; Teets, T. S.; Suntivich, J.; Shao-Horn, Y. *Chem. Sci.* **2010**, *1*, 411. (d) Dogutan, D. K.; Stoian, S. A; McGuire, R.;

Schwalbe, M.; Teets, T. S.; Nocera, D. G. *J. Am. Chem. Soc.* **2011**, *133*, 131. (e) Teets, T. S.; Cook, T. R.; McCarthy, B. D.; Nocera, D. G. *J. Am. Chem. Soc.* **2011**, *133*, 8114.
(23) (a) Askarizadeh, E.; Yaghoob, S. B.; Boghaei, D. M.; Slawin, A. M. Z.; Love, J. B. *Chem. Commun.* **2010**, *46*, 710. (b) Volpe, M.; Hartnett, H.; Leeland, J. W.; Wills, K.; Ogunshun, M.; Duncombe, B. J.; Wilson, C.; Blake, A. J.; McMaster, J.; Love, J. B. *Inorg. Chem.* **2009**, *48*, 5195.
(24) Ramdhanie, B.; Telser, J.; Caneschi, A.; Zakharov, L. N.; Rheingold, A. L.; Goldberg, D. P. *J. Am. Chem. Soc.* **2004**, *126*, 2515.
(25) Savéant, J.-M. *Chem. Rev.* **2008**, *108*, 2348.
(26) Schechter, A.; Stanevsky, M.; Mahammed, A.; Gross, Z. *Inorg. Chem.* **2012**, *21*, 22.
(27) (a) Chen, R.; Li, H.; Chu, D.; Wang, G. *J. Phys. Chem. C* **2009**, *113*, 20689. (b) Shi, Z.; Zhang, J. *J. Phys. Chem. C* **2007**, *111*, 7084.
(28) (a) Masa, J.; Ozoemena, K.; Schuhmann, W.; Zagal, J. H. *J. Porphyrins Phthalocyanines* **2012**, *16*, 762. (b) Zagal, J. H.; Gulppi, M.; Isaacs, M.; Cárdenas-Jirón, G.; Aguirre, M. J. *Electrochim. Acta* **1998**, *44*, 1349.
(29) Ward, A. L.; Elbaz, L.; Kerr, J. B.; Arnold, J. *Inorg. Chem.* **2012**, *51*, 4694.
(30) Liu, R.; von Malotki, C.; Arnold, L.; Koshino, N.; Higashimura, H.; Baumgarten, M.; Müllen, K. *J. Am. Chem. Soc.* **2011**, *133*, 10372.
(31) Yoshimoto, S.; Inukai, J.; Tada, A.; Abe, T.; Morimoto, T.; Osuka, A.; Furuta, H.; Itaya, K. *J. Phys. Chem. B* **2004**, *108*, 1948.
(32) (a) Hatay, I.; Su, B.; Li, F.; Méndez, M. A.; Khoury, T.; Gros, C. P.; Barbe, J.-M.; Ersoz, M.; Samec, Z.; Girault, H. H. *J. Am. Chem. Soc.* **2009**, *131*, 13453. (b) Partovi-Nia, R.; Su, B.; Li, F.; Gros, C. P.; Barbe, J.-M.; Samec, Z.; Girault, H. H. *Chem. Eur. J* **2009**, *15*, 2335. (c) Hatay, I.; Su, B.; Méndez, M. A.; Corminboeuf, C.; Khoury, T.; Gros, C. P.; Bourdillon, M.; Meyer, M.; Barbe, J.-M.; Ersoz, M.; Zális, S.; Samec, Z.; Girault, H. H. *J. Am. Chem. Soc.* **2010**, *132*, 13733.
(33) (a) Decréau, R. A.; Collman, J. P.; Hosseini, A. *Chem. Soc. Rev.* **2010**, *39*, 1291. (b) Collman, J. P.; Boulatov, R.; Sunderland, C. J.; Fu, L. *Chem. Rev.* **2004**, *104*, 561.
(34) (a) Rosenthal, J.; Nocera, D. G. *Acc. Chem. Res.* **2007**, *40*, 543. (b) Schwalbe, M.; Dogutan, D. K.; Stoian, S. A.; Teets, T. S.; Nocera, D. G. *Inorg. Chem.* **2011**, *50*, 1368. (c) Chang, C. J.; Chng, L. L.; Nocera, D. G. *J. Am. Chem. Soc.* **2003**, *125*, 1866.
(35) (a) Halime, Z.; Kotani, H.; Fukuzumi, S.; Karlin, K. D. *Proc. Natl. Acad. Sci. U.S.A.* **2011**, *108*, 13990. (b) Chufán, E. E.; Puiu, S. C.; Karlin, K. D. *Acc. Chem. Res.* **2007**, *40*, 563. (c) Kim, E.; Chufán, E. E.; Kamaraj, K.; Karlin, K. D. *Chem. Rev.* **2004**, *104*, 1077.
(36) (a) Carver, C. T.; Matson, B. D.; Mayer, J. M. *J. Am. Chem. Soc.* **2012**, *134*, 5444. (b) Matson, B. D.; Carver, C. T.; Von Ruden, A.; Yang, J. Y.; Raugei, S.; Mayer, J. M. *Chem. Commun.* **2012**, *48*, 11100. (c) Warren, J. J.; Tronic, T. A.; Mayer, J. M. *Chem. Rev.* **2010**, *110*, 6961.
(37) (a) Fukuzumi, S.; Kotani, H.; Lucas, H. R.; Doi, K.; Suenobu, T.; Peterson, R.; Karlin, K. D. *J. Am. Chem. Soc.* **2010**, *132*, 6874. (b) Tahsini, L.; Kotani, H.; Lee, Y.-M.; Cho, J.; Nam, W.; Karlin, K. D.; Fukuzumi, S. *Chem. Eur. J* **2012**, *18*, 1084. (c) Fukuzumi, S.; Tahsini, L.; Lee, Y.-M.; Ohkubo, K.; Nam, W.; Karlin, K. D. *J. Am. Chem. Soc.* **2012**, *134*, 7025.
(38) (a) Thorseth, M. A.; Letko, C. S.; Rauchfuss, T. B.; Gewirth, A. A. *Inorg. Chem.* **2011**, *50*, 6158. (b) Girth, A. A.; Thorum, M. S. *Inorg. Chem.* **2010**, *49*, 3557. (c) Thorum, M. S.; Yadav, J.; Gewirth, A. A. *Angew. Chem., Int. Ed.* **2009**, *48*, 165.
(39) McCrory, C. C. L.; Devadoss, A.; Ottenwaelder, X.; Lowe, R. D.; Stack, T. D. P.; Chidsey, C. E. D. *J. Am. Chem. Soc.* **2011**, *133*, 3696.
(40) Orzeł, Ł.; Kania, A.; Rutkowska-Żbik, D.; Susz, A.; Stochel, G.; Fiedor, L. *Inorg. Chem.* **2010**, *49*, 7362.
(41) Chen, C.-Y.; Sun, E.; Fan, D.; Taniguchi, M.; McDowell, B. E.; Yang, E.; Diers, J. R.; Bocian, D. F.; Holten, D.; Lindsey, J. S. *Inorg. Chem.* **2012**, *51*, 9443.
(42) Saga, Y.; Miura, R.; Sadaoka, K.; Hirai, Y. *J. Phys. Chem. B* **2011**, *115*, 11757.
(43) (a) Oettmeler, W.; Janson, T. R.; Thurnauer, M. C.; Shipman, L. L.; Katz, J. J. *J. Phys. Chem.* **1977**, *81*, 339. (b) Hartwich, G.; Fiedor, L.; Simonin, I.; Cmiel, E.; Schäfer, W.; Noy, D.; Scherz, A.; Scheer, H. *J. Am. Chem. Soc.* **1998**, *120*, 3675.
(44) Armarego, W. L. F.; Chai, C. L. L. In *Purification of Laboratory Chemicals*, 5th ed.; Butterworth-Heinemann: Oxford, U.K., 2003.
(45) (a) Wasielenski, M. R.; Svec, W. A. *J. Org. Chem.* **1980**, *45*, 1969. (b) Zheng, G.; Li, H.; Zhang, M.; L-Katz, S.; Chance, B.; Glickson, J. D. *Bioconjugate Chem* **2002**, *13*, 392. (c) Arian, D.; Cló, E.; Gothelf, K. V.; Mokhir, A. *Chem. Eur. J.* **2010**, *16*, 288. (d) Ishigure, S.; Mitsui, T.; Ito, S.; Kondo, Y.; Kawabe, S.; Kondo, M.; Dewa, T.; Mino, H.; Itoh, S.; Nango, M. *Langmuir* **2010**, *26*, 7774. (e) Paolesse, R.; Pandey, R. K.; Forsyth, T. P.; Jaquinod, L.; Gerzevske, K. R.; Nurco, D. J.; Sengo, M. O.; Licoccia, S.; Boschi, T.; Smith, K. M. *J. Am. Chem. Soc.* **1996**, *118*, 3869.
(46) (a) Tamiaki, H.; Kunieda, M. *J. Org. Chem.* **2007**, *72*, 2443. (b) Huber, V.; Sengupta, S.; Würthner, F. *Chem. Eur. J.* **2008**, *14*, 7791.
(47) (a) Ellis, P. E.; Linard, J. E.; Szymanski, T.; Jones, R. D.; Budge, J. R.; Basolo, F. *J. Am. Chem. Soc.* **1980**, *102*, 1889. (b) Hill, A. V. *J. Physiol. (London)* **1910**, *40*, 4.
(48) Fukuzumi, S.; Kuroda, S.; Tanaka, T. *J. Am. Chem. Soc.* **1985**, *107*, 3020.
(49) (a) Fukuzumi, S.; Imahori, H.; Yamada, H.; El-Khouly, M. E.; Fujitsuka, M.; Ito, O.; Guldi, D. M. *J. Am. Chem. Soc.* **2001**, *123*, 2571. (b) Fukuzumi, S.; Ohkubo, K.; Chen, Y.; Pandey, R. K.; Zhan, R.; Shao, J.; Kadish, K. M. *J. Phys. Chem. A* **2002**, *106*, 5105.
(50) Mann, C. K.; Barnes, K. K. In *Electrochemical Reactions in Non-aqueous Systems*; Marcel Dekker: New York, 1970.
(51) ESI-MS measurements have been performed to detect the $[Co^{II}(ChH)]^+$. However, no peak due to the protonated $Co^{II}(Ch)$ was observed because oxidation of $Co^{II}(Ch)$ to $[Co^{III}(Ch)]^+$ with $HClO_4$ occurred in the presence of a small amount of O_2 in the ESI-MS cavity.[19]
(52) (a) Honda, T.; Kojima, T.; Kobayashi, N.; Fukuzumi, S. *Angew. Chem., Int. Ed.* **2011**, *50*, 2725. (b) Honda, T.; Kojima, T.; Fukuzumi, S. *Chem. Commun.* **2011**, *47*, 7986.
(53) Bernstein, P. A.; Lever, A. B. P. *Inorg. Chim. Acta* **1992**, *198–200*, 543.
(54) Collman, J. P.; Berg, K. E.; Sunderland, C. J.; Aukauloo, A.; Vance, M. A.; Solomon, E. I. *Inorg. Chem.* **2002**, *41*, 6583.
(55) Ohkubo, K.; Kitaguchi, H.; Fukuzumi, S. *J. Phys. Chem. A* **2006**, *110*, 11613.
(56) (a) Fukuzumi, S.; Ohkubo, K. *Chem. Eur. J* **2000**, *6*, 4532. (b) Fukuzumi, S.; Patz, M.; Suenobu, T.; Kuwahara, Y.; Itoh, S. *J. Am. Chem. Soc.* **1999**, *121*, 1605. (c) Ohkubo, K.; Saija C. Menon, S. C.; Orita, A.; Otera, J.; Fukuzumi, S. *J. Org. Chem.* **2003**, *68*, 4720.
(57) The initial slow rise profile resulted from the mixing step of the solutions. The rate constants were determined from single-exponential curve fitting without the initial step.
(58) The saturated k_{obs} value is much smaller than the k_{obs} value of Me_2Fc in Figure 9. In such a case, the saturation behavior in Figure 13b may result from the complex formation between Br_2Fc and $[Co^{III}(ChH)]^{2+}$ prior to electron transfer.